

Supramolecular Patterns Controlled by Electron Interference and Direct Intermolecular Interactions

Yongfeng Wang,^{*,†} Xin Ge,[†] Carlos Manzano,[†] Jörg Kröger,[†] Richard Berndt,[†] Werner A. Hofer,[‡] Hao Tang,[§] and Jorge Cerda^{||}

Institut für Experimentelle und Angewandte Physik, Christian-Albrechts-Universität, D-24098 Kiel, Germany, Surface Science Research Center, University of Liverpool, Liverpool L69 3BX, United Kingdom, Centre d'Elaboration de Matériaux et d'Etudes Structurales, Centre National de la Recherche Scientifique, France, and Instituto de Ciencia de Materiales de Madrid Consejo Superior de Investigaciones Científicas, E-28049 Madrid, Spain

Received April 30, 2009; E-mail: yfwang@physik.uni-kiel.de

Surface-state electrons of (111) surfaces of noble metals are model systems for two-dimensional free electron gases. Scattering of electrons by adsorbed atoms or molecules leads to Friedel-type oscillations of the local density of surface states around the adsorbates,¹ which mediate an indirect long-range adsorbate–adsorbate interaction via the substrate.^{2,3} Large arrays of cerium on Ag(111) have been prepared using these surface state-mediated interactions.⁴ One-dimensional rows of pentacene on Cu(110) exhibited a specific intermolecular distance, which was tentatively attributed to a drastically modified surface state on Cu(110).⁵ To fabricate two-dimensional supramolecular architectures^{6–21} direct molecule–molecule interactions have been utilized, including dipole–dipole⁶ and metal–organic interactions,^{9,21} hydrogen bonding,^{10,14} and covalent interactions.¹⁶ However, two-dimensional molecular arrays based on substrate-mediated interaction via electron interference have not yet been reported.

Here, we present the fabrication of two-dimensional molecular arrays of cobalt–phthalocyanine (CoPc) on Cu(111) by combining electron interference patterns and substrate-induced directional molecule–molecule interactions. A long-range dispersed hexagonal pattern, an array of molecular chains, and a kagome network of phthalocyanines were prepared for the first time. In particular, the kagome lattice belongs to the symmetry group $p31m$, which has not been reported in two-dimensional organic crystals. In higher molecule layers, where electron interference is negligible, CoPc forms a close-packed structure through weak intermolecular C–H...N hydrogen bonds. Similarly, CoPc on the less reactive Ag(111) surface exhibits simple close-packed tetragonal patterns. Modeling based on first-principles calculations corroborates the interpretation of the experimental results.

CoPc exhibits a 4-fold symmetry (C_4) according to density functional theory (DFT) (Supporting Information, Figure S1), which is similar to that found in three-dimensional molecular crystals by X-ray diffraction. Low-temperature scanning tunneling microscopy (STM) (Figure 1a) reveals that adsorption onto the 3-fold symmetric Cu(111) surface reduces the molecular symmetry to 2-fold (C_2).²² A symmetry reduction from C_4 to C_2 is also obvious for SnPc molecules on Ag(111) (Figure 1b).²³

Calculated relaxed geometries of CoPc on Cu(111) (Supporting Information, Figure S1) and of SnPc on Ag(111)²³ (Figure 1c)

further support these observations and reveal that the atomic positions within the two perpendicular axes of the molecule are different.

As a consequence, we suggest that the charge transfer between substrate and molecule is likewise different for the two pairs of

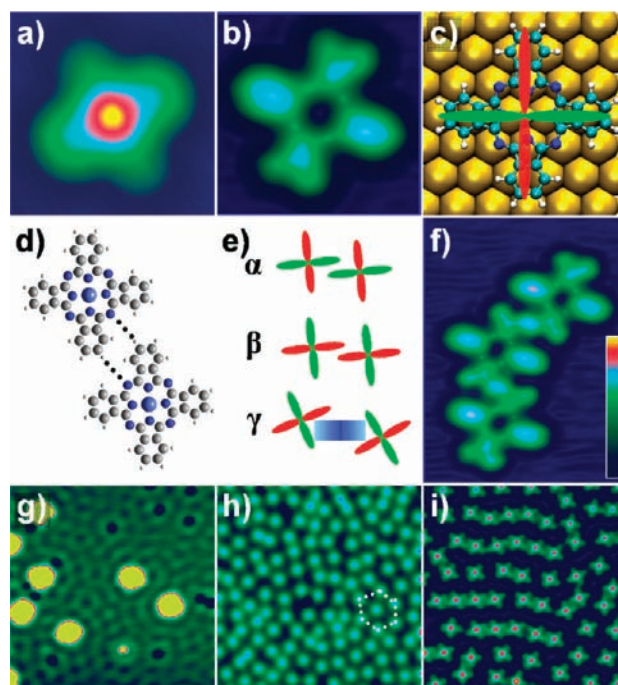


Figure 1. Constant-current STM images of (a) CoPc on Cu(111) ($2 \text{ nm} \times 2 \text{ nm}$, -0.6 V) and (b) SnPc on Ag(111) with Sn oriented toward the substrate (Sn-down, $2 \text{ nm} \times 2 \text{ nm}$, -0.03 V). Molecular lobes appear split along the^{1–10} substrate direction. (c) Relaxed geometry of SnPc on Ag(111) with Sn-down configuration (Supporting Information, theoretical simulations for SnPc on Ag(111)). The superimposed red/green cross denotes split/unsplit lobes or larger/smaller partial charge transfer between Ag(111) and SnPc, respectively. (d) Schematics of a molecular dimer with weak C–H...N hydrogen bonds. (e) Three dimer configurations. Dimer α is coupled via H-bonds, while dimer γ is stabilized by surface state-mediated interaction. Dimer β was not observed. (f) STM image of a Sn-down trimer ($3 \text{ nm} \times 4 \text{ nm}$, -0.05 V) formed along the split lobes (green part of the cross). (g) STM image of standing wave patterns around CoPc on Cu(111) ($20 \text{ nm} \times 20 \text{ nm}$, -0.6 V). (h) 0.5 ML CoPc on Cu(111) ($25 \text{ nm} \times 25 \text{ nm}$, -1.0 V). Typical intermolecular distance is 2.1 nm. (i) Coexistence of dispersed molecules (predominant distance 2.1 nm) and molecular chains (interchain distance 2.1 nm, intrachain distance 1.5 nm) (0.55 ML, $16 \text{ nm} \times 16 \text{ nm}$, -1.0 V). The protrusion at the center of CoPc in STM images is bias dependent (Supporting Information, Figure S1). The color scale bar for the STM images is shown in (f).

[†] Christian-Albrechts-Universität.

[‡] University of Liverpool.

[§] Centre National de la Recherche Scientifique.

^{||} Instituto de Ciencia de Materiales de Madrid Consejo Superior de Investigaciones Científicas.

molecule ligands. In Figure 1c this difference is indicated by the colors of the ligand pairs. Green represents ligands along the close-packed substrate direction, and red those along the perpendicular direction. In STM images (Figure 1b) the “green lobes” appear as split protrusions, which are attributed to a reduced charge transfer between Ag(111) and SnPc. Similarly, red parts denote a larger charge transfer and correspond to single lobes in STM images. Below, we use this “green-red cross” to represent the reduced symmetry of adsorbed SnPc and CoPc molecules.

The reduced symmetry has consequences for molecular dimers which are stabilized by weak C–H...N hydrogen bonds²⁴ (dashed lines in Figure 1d). As these bonds may involve both types of ligands, different dimers (α and β in Figure 1e) may be formed. Furthermore, long-range interactions mediated by the quantum interference of surface state electrons can also stabilize a molecular dimer (γ , Figure 1e). STM images reveal that SnPc molecules adsorbed with Sn oriented toward the surface (Sn-down) form peculiar chain structures. In these chains, the interaction between the constituents occurs via split lobes (Figure 1f).

For low coverages ($\theta < 0.5$ ML, one monolayer (ML) is defined by one CoPc molecule per 38 copper atoms, the most dense structure observed), CoPc molecules on Cu(111) remain separated from each other and standing wave patterns around CoPc are clearly visible (Figure 1g). The surface charge density variations associated with the patterns mediate long-range interactions between atoms and molecules.²⁵ Indeed, histograms of the nearest-neighbor separations of CoPc at $\theta < 0.5$ ML indicate preferred distances of 2.1, 3.6, 5.0, and 6.5 nm (Supporting Information, Figures S2, S3). The differences between these separations match half the Fermi wavelength of the Cu(111) surface state as expected for surface state mediated interaction (2). At coverages slightly above 0.5 ML, we do not find a uniform compression of the intermolecular distances, a scenario which would be indicative of (surface-enhanced) dipole–dipole interactions²⁶ or electrostatic repulsion between molecules.²⁷ Rather, CoPc forms one-dimensional chains. These observations indicate that the surface state is essential in the formation of self-assembled structures. Moreover, the coverage-controlled formation of first γ and next α dimers (Figure 1h,i) suggests a sequence of binding energies $E(\gamma) > E(\alpha) > 0$.

The above sequence of energies is useful to analyze further data on the coverage-dependent self-assembly. At $\theta \approx 0.5$ ML, molecules form a pattern with local hexagonal symmetry ($p6$) (Phase h , Figure 1h). The distance between two neighboring molecules is ~ 2.1 nm (dimer γ). This structure is similar to Cu atom assemblies on Cu(111)² and Br island arrays on Cu(111),²⁶ which are both stabilized by the quantum interference of surface state electrons. At 0.7 ML, CoPc forms an array of chains (Figure 2a, phase a , $p2$) with a unique distance between adjacent chains of, again, 2.1 nm. Phase a is composed of dimers γ and α . The molecules form close-packed dimers exclusively along “green” lobes (Figure 2a). Six kinds of domains for phase a are observed, which reflect three azimuthal orientations and their mirror images (Supporting Information, Figure S4). Upon increasing the coverage to 0.8 ML, the molecular superstructure evolves into an unusual kagome network (Figure 2b, Phase b). Once again, an intermolecular distance of 2.1 nm (Figure 2b, dashed triangle) is observed indicating that Phase b is most likely stabilized by surface state-mediated interactions. Detailed inspection shows that Phase b exhibits the unexpected highly symmetric plane group $p31m$ (Figure 3). We suggest that a combination of surface state-mediated and intermolecular interactions are at the origin of this peculiar superstructure. The intricate balance of these interactions results in the large unit cell containing two molecules (Table 1) with

dimensions $2.8 \text{ nm} \times 2.8 \text{ nm}$. Owing to 3-fold rotational symmetry and mirror planes, there are only two kinds of domains, one shown in Figure 2b, another one rotated by 60° .

Beyond a coverage of 0.8 ML, the molecules are forced to approach closer than the characteristic distance of surface state-mediated interaction. As a result, direct intermolecular interactions start to dominate the assembly and lead to close-packed structures at 1.0 ML (Figure 2c, phase c , $p2$, and Figure 2d, phase d , $p2$). These dense structures would require CoPc to arrange as β dimers, which are not found in molecular chains. In the monolayer, β configurations of CoPc are avoided in two ways. In Figure 2c, some

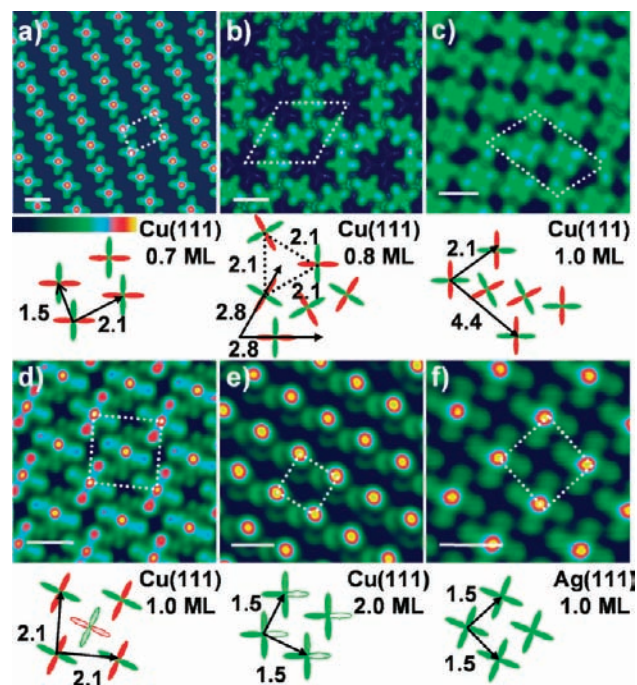


Figure 2. STM images and schematic models of superstructure of CoPc on Cu(111) and Ag(111) and CoPc monolayer on Cu(111) reveal six phases. Below 1.0 ML, CoPc molecules form ordered arrays of chains ((a), 0.7 ML, -0.5 V), and a kagome network ((b), 0.8 ML, 0.2 V) on Cu(111). The color scale bar for STM images is shown in (a). At ~ 1.0 ML, CoPc assembles into two new superstructures. Either some molecules are rotated by 30° ((c), 0.2 V) or an alternating pattern with 2 molecules per unit cell is formed, which reflect different adsorption configurations ((d), $6 \text{ nm} \times 6 \text{ nm}$, -0.6 V). Two simplified models with different color depths denote two different adsorption geometries in (d). On a CoPc monolayer supported by Cu(111) or Ag(111), CoPc aggregates into a single ordered structure ((e), 1.2 ML, -1.0 V; (f), 1.0 ML, -0.6 V). Different saturations of the lobe colors in the schematics in (e) indicate an $\sim 3^\circ$ tilt of molecules in the second layer with respect to the substrate plane. The C_4 symmetry of CoPc on Ag(111) is represented by a “green–green cross” in (f). White scale bars in all images denote 1.5 nm.

Table 1. Structures of Adsorption Phases of CoPc on Cu(111)^a

phase	h	a	b	c	d	e	f
molecules per unit cell	1	1	3	3	2	1	1
point group of CoPc	C_2	C_2	C_2	C_2	C_2	C_1	C_4
plane group (2D crystal)	$p6$	$p2$	$p31m$	$p2$	$p2$	$p1$	$p4$
domain (total 39)	1	6	2	6	6	12	6

^a For the phases defined in Figures 1h and 2a–f, the number of molecules per unit cell, the point group of the symmetry-reduced adsorbed molecule, the plane group of the two-dimensional (2D) molecular pattern, and the number of equivalent domains on the Cu(111) substrate are listed.

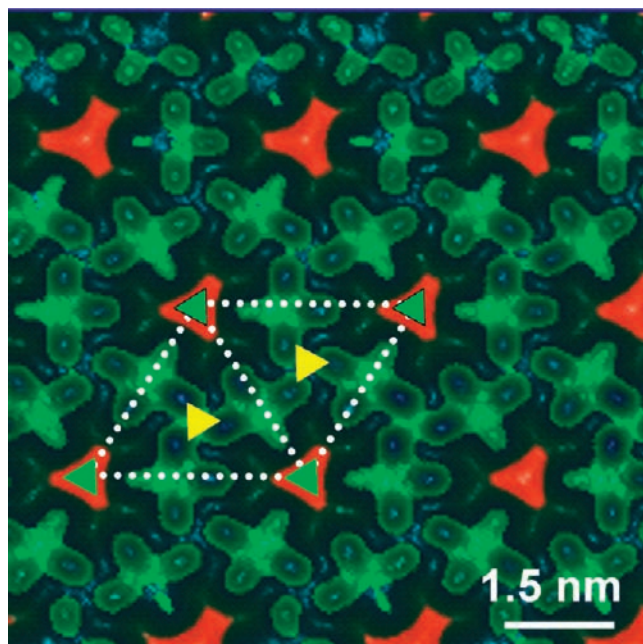


Figure 3. Image from Figure 2b represented with an inverted color scale to emphasize symmetry elements. White dotted lines denote mirror axes. Rotation axes on mirror axes and elsewhere are indicated by green and yellow triangles, respectively. The plane group is $p31m$.

of the molecules are rotated by 30° with respect to their direct neighbors, which effectively increases the distance between “red” lobes and leads to a large unit cell with three molecules (Table 1). In Figure 2d, CoPc adopts two alternating adsorption configurations to minimize repulsion between “red” lobes.

In the second molecule layer, CoPc molecules are partially decoupled from the metallic Cu surface. As a result, ordered two-dimensional islands aggregate on Cu(111) at low coverages ($\theta \approx 1.2$ ML) with only stable dimers of type α (Figure 2e, phase e). Molecules in the second layer are tilted $\sim 3^\circ$ with respect to the substrate,²³ which reduces the symmetry of CoPc from C_4 to C_1 , and the plane symmetry group changes to $p1$. Upon changing the substrate from Cu(111) to Ag(111), CoPc shows its original C_4 symmetry and forms only regular ordered patterns (Figure 2f, phase f , $p4$), which is similar to reported superstructures formed by Pc on inert metals.^{28,29} Only dimer α is observed in the STM images.

Obviously, the surface plays an important role in controlling the molecular superstructures.³⁰ First, CoPc molecules prefer to lie flat on metallic surfaces to maximize the interaction between their π -electrons and the surface. Second, two lobes of a molecule orient along the close-packed substrate direction to maximize their interaction. Third, molecules prefer to form one-dimensional structures at low coverages owing to the symmetry reduction of molecules. Fourth, the quantum interference of surface state electrons is essential for the formation of disperse ordered self-assembled structures (phases h , a , and b).

In summary, two-dimensional crystals of CoPc with plane symmetry groups $p1$, $p2$, $p4$, local $p6$, and, for the first time, $p31m$

have been fabricated by utilizing a combination of quantum interference of surface state electrons, directional molecule–molecule attraction caused by symmetry reduction, and substrate–molecule interaction. This combination of interactions provides opportunities to induce new structures with high symmetry and can be adapted to a wide range of molecules.

Acknowledgment. Financial support by the Deutsche Forschungsgemeinschaft through SFB 677 is gratefully acknowledged. W.A.H. thanks the Royal Society, London. J.C. acknowledges financial support from the Spanish Ministry of Science and Technology under Project MAT2007-66719-C03-02. H.T. acknowledges computational resources provided by CALMIP.

Supporting Information Available: Experimental section, theoretical simulations for SnPc on Ag(111) and CoPc on Cu(111), relaxed adsorption geometry and simulated STM images of CoPc on Cu(111), histograms of the nearest-neighbor separations of CoPc at $\theta \approx 0.06$ ML and 0.55 ML, and six types of domains of phase a . This material is available free of charge via the Internet at <http://pubs.acs.org>.

References

- (1) Crommie, M. F.; Lutz, C. P.; Eigler, D. M. *Nature* **1993**, *363*, 524.
- (2) Repp, J.; Moresco, F.; Meyer, G.; Rieder, K. H.; Hyldgaard, P.; Persson, M. *Phys. Rev. Lett.* **2000**, *85*, 2981.
- (3) Knorr, N.; Brune, H.; Epple, M.; Hirstein, A.; Schneider, M. A.; Kern, K. *Phys. Rev. B* **2002**, *65*, 115420.
- (4) Silly, F.; Pivetta, M.; Ternes, M.; Patthey, F.; Pelz, J. P.; Schneider, W. D. *Phys. Rev. Lett.* **2004**, *92*, 016101.
- (5) Lukas, S.; Witte, G.; Wöll, C. *Phys. Rev. Lett.* **2002**, *88*, 028301.
- (6) Böhringer, M.; Schneider, W.-D.; Berndt, R. *Angew. Chem., Int. Ed.* **2000**, *39*, 792.
- (7) Corso, M.; Auwärter, W.; Muntwiler, M.; Tamai, A.; Greber, T.; Osterwalder, J. *Science* **2004**, *303*, 217.
- (8) Stöhr, M.; Wahl, M.; Galka, C. H.; Riehm, T.; Jung, T. A.; Gade, L. H. *Angew. Chem., Int. Ed.* **2005**, *44*, 7394.
- (9) Barth, J. V. *Annu. Rev. Phys. Chem.* **2007**, *58*, 375.
- (10) Wan, L. J. *Acc. Chem. Res.* **2006**, *39*, 334.
- (11) De Feyter, S.; De Schryver, F. C. *Chem. Soc. Rev.* **2003**, *32*, 393.
- (12) Néel, N.; Kröger, J.; Berndt, R. *Appl. Phys. Lett.* **2006**, *88*, 163101.
- (13) Néel, N.; Kröger, J.; Berndt, R. *Adv. Mater.* **2006**, *18*, 174.
- (14) Ye, Y. C.; Sun, W.; Wang, Y. F.; Shao, X.; Xu, X. G.; Cheng, F.; Li, J. L.; Wu, K. J. *J. Phys. Chem. C* **2007**, *111*, 10138.
- (15) Kröger, J.; Jensen, H.; Berndt, R.; Rurali, R.; Lorente, N. *Chem. Phys. Lett.* **2007**, *438*, 249.
- (16) Grill, L.; Dyer, M.; Lafferentz, L.; Persson, M.; Peters, M. V.; Hecht, S. *Nat. Nanotechnol.* **2007**, *2*, 687.
- (17) Vang, R. T.; Lauritsen, J. V.; Laegsgaard, E.; Besenbacher, F. *Chem. Soc. Rev.* **2008**, *37*, 2191.
- (18) Schull, G.; Becker, M.; Berndt, R. *Phys. Rev. Lett.* **2008**, *101*, 4.
- (19) Pivetta, M.; Blum, M. C.; Patthey, F.; Schneider, W.-D. *Angew. Chem., Int. Ed.* **2008**, *47*, 1076.
- (20) Blunt, M. O.; Russell, J. C.; Gimenez-Lopez, M. D.; Garrahan, J. P.; Lin, X.; Schroder, M.; Champness, N. R.; Beton, P. H. *Science* **2008**, *322*, 1077.
- (21) Barth, J. V.; Costantini, G.; Kern, K. *Nature* **2005**, *437*, 671.
- (22) Chang, S. H.; Kuck, S.; Brede, J.; Lichtenstein, L.; Hoffmann, G.; Wiesendanger, R. *Phys. Rev. B* **2008**, *78*, 233409.
- (23) Wang, Y. F.; Kröger, J.; Berndt, R.; Hofer, W. *Angew. Chem., Int. Ed.* **2009**, *48*, 1261.
- (24) Wang, Y. F.; Ge, X.; Schull, G.; Berndt, R.; Bornholdt, C.; Koehler, F.; Herges, R. *J. Am. Chem. Soc.* **2008**, *130*, 4218.
- (25) Kamna, M. M.; Stranick, S. J.; Weiss, P. S. *Science* **1996**, *274*, 118.
- (26) Nanayakkara, S. U.; Sykes, E. C. H.; Fernandez-Torres, L. C.; Blake, M. M.; Weiss, P. S. *Phys. Rev. Lett.* **2007**, *98*, 206108.
- (27) Fernandez-Torres, L.; Monturet, S.; Franke, K. J.; Fraxedas, J.; Lorente, N.; Pascual, J. I. *Phys. Rev. Lett.* **2007**, *99*, 4.
- (28) Cheng, Z. H.; Gao, L.; Deng, Z. T.; Liu, Q.; Jiang, N.; Lin, X.; He, X. B.; Du, S. X.; Gao, H. J. *J. Phys. Chem. C* **2007**, *111*, 2656.
- (29) Suto, K.; Yoshimoto, S.; Itaya, K. *J. Am. Chem. Soc.* **2003**, *125*, 14976.
- (30) Wang, Y. F.; Ye, Y. C.; Wu, K. J. *J. Phys. Chem. B* **2006**, *110*, 17960.

JA903506S